Low-energy electron scattering by C_2HF_5

M. H. F. Bettega
Departamento de Física, Universidade Federal do Paraná, Caixa Postal 19044, 81531-990, Curitiba, Paraná, Brazil and A. A. Noyes Laboratory of Chemical Physics, California Institute of Technology, Pasadena, California 91125

C. Winstead and V. McKoy
A. A. Noyes Laboratory of Chemical Physics, California Institute of Technology, Pasadena, California 91125

(Received 23 October 2000; accepted 9 January 2001)

We report elastic and electronically inelastic cross sections for low-energy electron scattering by pentafluoroethane, C_2HF_5. Our calculations were performed using the Schwinger multichannel method. For elastic scattering, we calculated integral, differential, and momentum transfer cross sections for energies from 5 to 50 eV. In the inelastic case, we obtained integral and differential cross sections for electron-impact excitation of the $1\,^{1,3}A'$ and $2\,^{1,3}A'$ excited states at the three-channel level of approximation. At higher energies, the elastic differential cross sections are quite similar to existing theoretical results for C_2F_6. Limited electronic-structure calculations were carried out to explore the dissociation behavior of the excited states. © *2001 American Institute of Physics.* [DOI: 10.1063/1.1352037]

I. INTRODUCTION

Electron–molecule collisions at low impact energies (i.e., at energies from less than 1 eV up to a few tens of eV) play a major role in semiconductor processing plasmas. Electronically inelastic and ionizing collisions are principally responsible for generating reactive charged and neutral fragment species that drive chemical and physical change at the semiconductor surface, while electronically elastic collisions affect electron transport and the rate of energy deposition. Moreover, the energies and widths of elastic shape resonances give some indication of the probabilities for resonant vibrational excitation and dissociative attachment, even without explicit computation of cross sections for those channels. For these reasons, elastic and electronically inelastic electron collision cross section information is valuable in the modeling of plasmas, yet such information is often unavailable for the molecules of interest.

Studies of low-energy collisions with polyatomic molecules are also of interest from a purely scientific standpoint. One line of inquiry is to explore systematics in electron collisions with related polyatomic molecules. In the case of the fluoro- and hydrofluorocarbons, for example, one might explore variations in the number and location of resonances or the magnitude of the cross section as a function of the size of the molecule or the degree of halogenation. Although some studies along these lines exist (e.g., Refs. 1–7), there is much work left to be done. As part of a projected series of articles, the present study of pentafluoroethane (C_2HF_5, also known as R125 or HFC-125) is intended to contribute to an understanding of trends in the low-energy electron cross sections of the $C_xH_yF_z$ molecules.

Because they degrade more quickly in the atmosphere than perhalocarbons, hydrofluorocarbons such as pentafluoroethane have been widely studied as alternative refrigerants. Within the semiconductor industry, the same environmental advantages have recently led to consideration of C_2HF_5 and other hydrofluorocarbons as precursor gases in the plasma deposition of polymeric fluorocarbon layers used as low-dielectric-constant insulators.[8] Detailed models of processing plasmas require cross section data for the principal low-energy electron collision processes, including elastic scattering, electron-impact excitation, electron-impact ionization, and dissociative attachment. However, little information concerning the electron collision properties of C_2HF_5 is available. Indeed, to our knowledge neither experimental nor theoretical values are available for the total scattering, elastic, electron-impact excitation, or dissociative attachment cross sections, and the electron-impact ionization cross section has only recently been measured.[9]

In the present work, we report calculations of electronically elastic electron scattering by C_2HF_5 between 5 and 50 eV, including differential, integral, and momentum-transfer cross sections. These calculations, carried out using the Schwinger multichannel (SMC) method,[10] employed the fixed-nuclei (FN) static-exchange (SE) approximation, i.e., polarization of the molecular charge density by the projectile electron was neglected. Although both the FN and the SE approximations introduce errors in the computed cross sections, those errors follow a regular pattern and can to some extent be discounted. We also report cross sections for four electron-impact excitation processes in C_2HF_5, computed using a few-channel description and the FN approximation. In conjunction with these inelastic cross section calculations, we have carried out limited studies of the excited states' potential-energy surfaces in order to determine whether the excited states are dissociative and if so into which products.

The remainder of the article is organized as follows. The theoretical method and computational details are described in Sec. II. Results are and discussion are contained in Sec. III. Concluding remarks are found in Sec. IV.

II. COMPUTATIONAL PROCEDURES

To compute the scattering cross sections, we have used the Schwinger multichannel (SMC) method[10,11] as implemented for parallel computers.[12] This method has been described in detail in previous publications, and we will not repeat that description here. The implementation for parallel computers has been reviewed recently.[13] All calculations were carried out in the FN approximation at the experimental equilibrium geometry,[14] which belongs to the C_s symmetry point group.

The C_2HF_5 molecule possesses a large permanent dipole moment. Because we employ a square-integrable (L^2) expansion of the wave function, scattering at large impact parameter via the dipolar component of the electron–molecule potential is not fully included; as a result, the partial-wave expansion of the scattering amplitude lacks high partial-wave terms that are necessary to describe correctly the near-forward scattering. In order to recover the long-range scattering from the dipole potential, we therefore ''completed'' the scattering amplitude by supplementing low partial-wave information obtained from the SMC calculation with high partial-wave information obtained by applying the first Born approximation to the dipole potential. In practice, we constructed a combined scattering amplitude by subtracting from the plane-wave representation of the dipole–Born amplitude terms up to some l_{SMC} and $|m_{\mathrm{SMC}}|$ in its partial-wave expansion and adding back corresponding partial-wave terms obtained from the SMC calculation; to obtain the differential cross section (DCS), the resulting amplitude was then expanded up to $l=10$ and averaged over directions of impact. For each impact energy, we chose the pair $(l_{\mathrm{SMC}},|m_{\mathrm{SMC}}|)$ that produced the least difference between the corrected DCS and the uncorrected SMC DCS at angles above 20°–30°; for example, at 5 eV we chose (6,2) and at 10 eV we chose (8,5). In general, $(l_{\mathrm{SMC}},|m_{\mathrm{SMC}}|)$ ranged from (6,2) to (9,8). Divergence of the DCS at 0°, and hence of the integral cross section (ICS), was avoided by including a small inelasticity, so that the momentum-transfer vector $\vec{q}=\vec{k}_f-\vec{k}_i$ occurring in the denominator of the dipole–Born scattering amplitude does not vanish. Details of the Born correction procedure employed in this work have been given elsewhere.[15]

Because singlet–singlet electronic transitions in C_2HF_5 are allowed by dipole selection rules, there is a contribution to their electron-impact excitation cross sections from the long-range interaction of the projectile with the transition dipole that is analogous to the contribution just described of the permanent dipole moment to the elastic cross section.[16] The same Born correction procedure can be employed in the inelastic case to account for this effect; however, we chose not to apply that correction to the results presented below. Single-excitation configuration interaction (CI) calculations using GAUSSIAN 94 (Ref. 17) and the 6-311++G(2d,2p) basis set, denoted for later reference as CIS/6-311++G(2d,2p), yielded oscillator strengths for the $X\,^1A'\rightarrow 1\,^1A'$ and $X\,^1A'\rightarrow 2\,^1A'$ transitions of 0.0878 and 0.0123, respectively. These values indicate that the omitted correction should be small for the $2\,^1A'$ state; for the $1\,^1A'$ state, the correction would be significant at the higher end of the energy range considered (threshold to 40 eV), but still modest at the lower impact energies that are of primary interest.

A. Elastic calculations

Our elastic calculations were performed within the fixed-nuclei, static-exchange approximation. The basis set used to describe the ground electronic state was the TZV++(2d,2p) basis set internal to the electronic structure program GAMESS.[18] The ground-state wave function was of the restricted Hartree–Fock (RHF) type. We obtained a value for the ground-state electric dipole moment of 1.786,D which compares well with the experimental values of 1.54D[19] and 1.563.D[20] The same basis set was used to describe the scattering system in the SMC calculations. As a check on our results, we also carried out scattering calculations using the 6-311++g(2d,2p) basis set, which is a bit smaller than the TZV++(2d,2p) set. We found no significant differences between the cross sections obtained with these two basis sets. It should be noted that GAMESS, unlike GAUSSIAN, retains all six Cartesian components of the d orbitals in these basis sets. Thus the TZV++(2d,2p) set for C_2HF_5 comprises a total of 220 contracted Gaussian functions and the 6-311++g(2d,2p) set comprises 213 contracted Gaussians.

B. Inelastic calculations

The inelastic cross sections were obtained from two separate three-channel calculations, the first including the $X\,^1A'$ ground state and the $1\,^3A'$ and $1\,^1A'$ excited states, the second including the ground state together with the $2\,^3A'$ and $2\,^1A'$ states. The basis set used in these calculations was 6-311++g(2d,2p).

To describe the triplet excited states, we performed a restricted single-excitation configuration interaction (SECI) calculation using GAMESS, permitting excitations only from the highest occupied molecular orbital, which belongs to the a' representation of C_s, and only into virtual orbitals of the same symmetry. The excitation energies obtained with this procedure were 11.926 eV for the $1\,^3A'$ state and 12.834 eV for the $2\,^3A'$ state. For singlet excited states (and a singlet ground state), Brillouin's theorem ensures that such a restricted SECI calculation is precisely equivalent to the improved virtual orbital (IVO) approximation.[21] Also, orthogonality considerations imply that such a calculation is precisely equivalent to an IVO calculation for a triplet excited state, unless (as in the present case) the hole and particle orbitals involved belong to the same irreducible representation, in which case some degree of relaxation of the hole orbital is included. However, after we reorthogonalized the natural orbital describing the excited state to the highest occupied RHF orbital from the ground state, the resulting single configuration description of the triplet excited state was of approximately IVO quality.

The current implementation of the SMC procedure requires a single configuration description of each target electronic state, with the orbitals for all states drawn from a common set. Thus the singlet excited states were described by the same configurations as the corresponding triplets, with only the spin coupling changed. We obtained excitation energies of 12.311 eV for the $1\,^1A'$ state and 13.283 eV for the

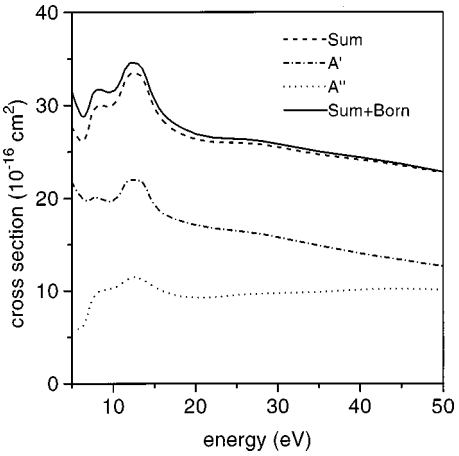

FIG. 1. Integral elastic electron-scattering cross section for C_2HF_5.

$2\,^1A'$ state using these wave functions. Because the particle orbitals were optimized for the triplet states, we expect that the singlet states and their thresholds will be somewhat less well described in our calculations. However, comparison with the unrestricted CIS/6-311++G($2d$,$2p$) calculations indicates that the qualitative description of the singlet states should still be correct, in that the leading configurations in the CIS/6-311++G($2d$,$2p$) wave function of each state arise from excitations out of the highest occupied orbital, and similar excitation thresholds are obtained (11.836 and 12.764 eV, respectively).

III. RESULTS AND DISCUSSION

A. Elastic scattering

In Fig. 1, we present the elastic integral cross section of C_2HF_5 along with its decomposition into the A' and A'' representations of the C_s point group. As may be seen, both representations contribute to the maxima in the integral cross section at about 7 and 13 eV. Figure 1 also shows the integral cross section that is obtained by the Born correction procedure described in the preceding section, which complements low partial-wave contributions to the scattering amplitude obtained via the SMC method with high partial-wave contributions computed via the first Born approximation applied to the dipole potential. The Born correction affects only the magnitude of the integral cross section at lower energies and not the shape.

In Fig. 2, we present the differential cross sections (DCS) for elastic scattering by C_2HF_5 at collision energies of 5 and 7.5 eV. At these energies, we have included the contribution of the dipole potential, which produces the enhanced forward scattering below about 20°. Figures 3 and 4 show the DCS at selected energies from 10 to 50 eV. At these energies, we have omitted the contribution of the dipole potential, which is only significant at extreme forward angles. For purposes of comparison, we also show in Figs. 3 and 4 results of a calculation on C_2F_6.[22,23] At 10 eV, the DCS of C_2F_6 exhibits a local maximum near 90° that is not seen in the DCS of C_2HF_5; however, at 15 and 20 eV the resemblance between the DCS for the two molecules is closer, and at 30 eV the two cross sections are very similar.

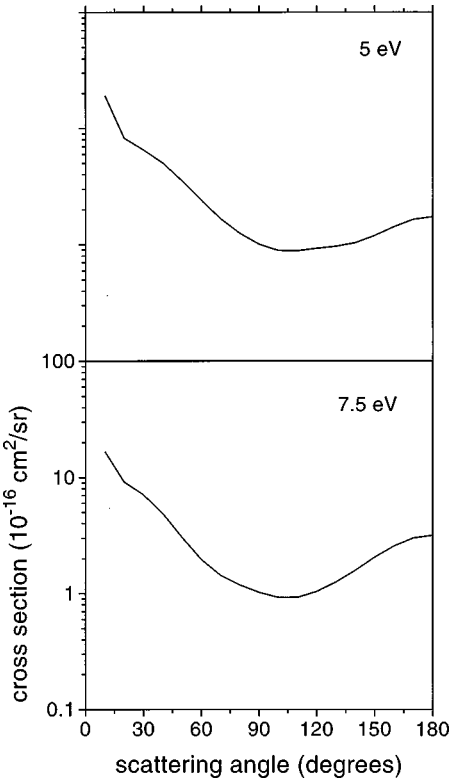

FIG. 2. Differential cross section for C_2HF_5 at 5 and 7.5 eV. At these energies, the Born correction is included.

It thus appears that the replacement of one fluorine by hydrogen has little effect on the elastic scattering at higher collision energies.

In Fig. 5, we show the momentum transfer cross section (MTCS) of C_2HF_5. Because the Born correction affects

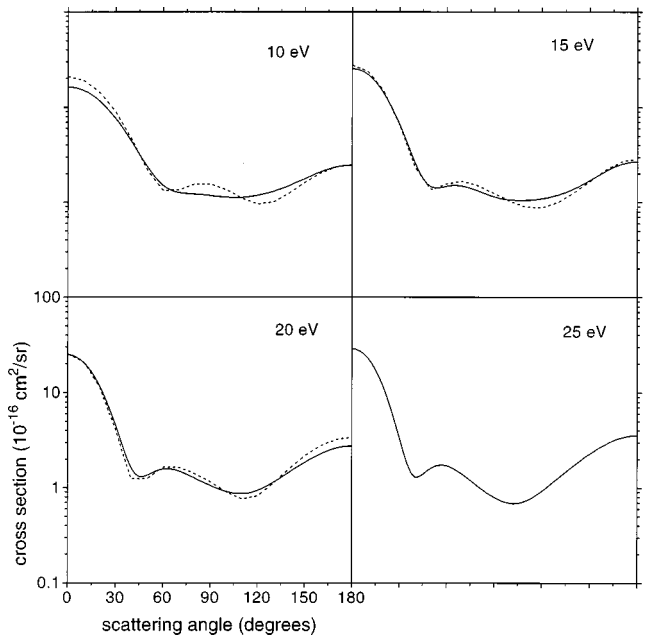

FIG. 3. Differential cross section for C_2HF_5 at 10, 15, 20, and 25 eV (solid lines). We also show the differential cross section for C_2F_6 at 10, 15, and 20 eV (dashed lines).

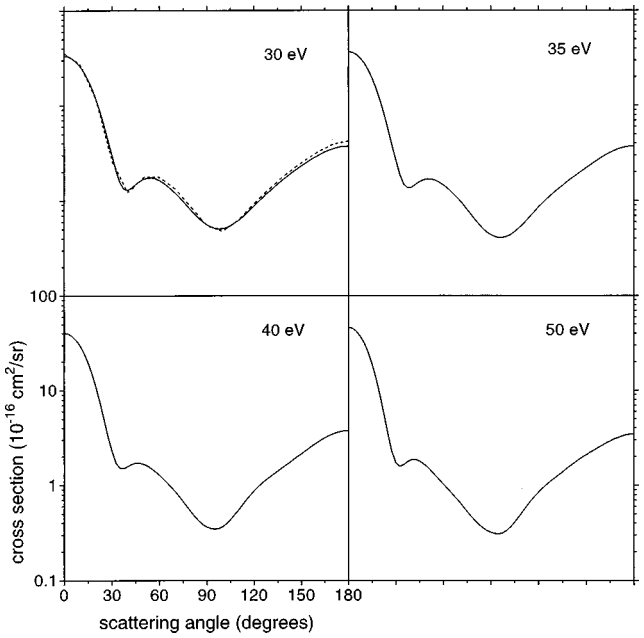

FIG. 4. Differential cross section for elastic scattering by C_2HF_5 at 30, 35, 40, and 50 eV (solid lines). Also shown is the differential cross section for C_2F_6 at 30 eV (dashed lines).

mostly the near-forward scattering, it has little influence on the MTCS; consequently, the results shown in Fig. 5 omit this correction.

Because neither experimental nor previous calculated elastic electron collision cross sections are, to our knowledge, available for C_2HF_5, it is difficult to assess directly the quality of the present results. However, insofar as the present results agree well with those computed for the closely related molecule C_2F_6, which in turn compare favorably to experimental data on C_2F_6 (Ref. 24) at higher energies, we have reason to believe that they represent well the scattering behavior of C_2HF_5 at those same energies. Conversely, at lower energies—roughly speaking, from the location of the double maximum in Fig. 1 downward—we expect the static-exchange approximation to work less well, although given the large dipole moment of C_2HF_5 we expect the dipole potential rather than the polarization potential to dominate the electron–target interaction at long range.[25–27] Because resonances are sensitive to short-range polarization effects, which are net attractive, we expect that the peaks in our cross section appear somewhat too high in energy; also, the rise in the A' component seen at the lowest energies in Fig. 1 is artifactual. It is also important to note that, in the related fluorocarbon CF_4, similar resonant peaks are seen in the fixed-nuclei elastic cross sections computed by various methods,[28–31] but not in the measured vibrationally elastic cross section;[32,33] rather, in CF_4 one finds strong resonant enhancement of the vibrationally inelastic cross sections[32,34] in the relevant energy range. We therefore speculate that much, if not most of the resonant enhancement of the C_2HF_5 FN elastic cross section, may likewise contribute to vibrational excitation.

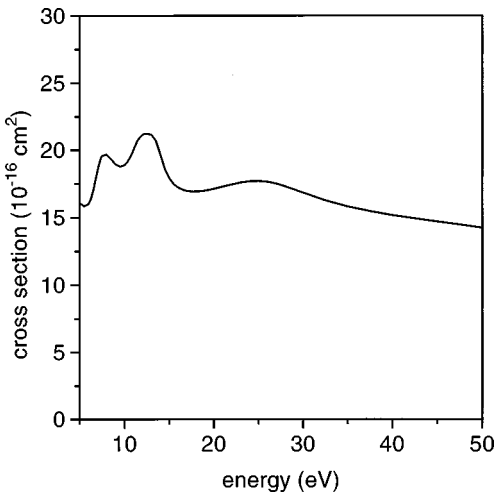

FIG. 5. Momentum transfer cross section for C_2HF_5.

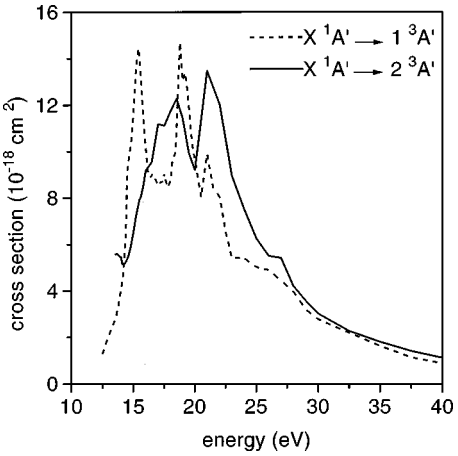

FIG. 6. Computed integral cross sections for electron-impact excitation to the $1\,^3A'$ (dashed line) and $2\,^3A'$ (solid line) excited states of C_2HF_5.

B. Electron-impact excitation

Figure 6 shows the integral excitation cross sections from the ground state $X\,^1A'$ to the $1\,^3A'$ and $2\,^3A'$ excited states of C_2HF_5. The peaks seen in the $1\,^3A'$ excitation cross section occur primarily in A' symmetry, with small contributions from A''. For the $2\,^3A'$ excitation cross section, the lower peak is associated with A' symmetry and the higher peak is associated with A''. Because we did not include closed channels in the calculation, the most likely explanation for these peaks is in terms of core-excited shape resonances. Figures 7 and 8 show the corresponding differential excitation cross sections at selected energies.

We studied the behavior of the $1\,^3A'$ and $1\,^3A'$ states following electron-impact excitation by carrying out geometry optimizations using SECI wave functions, denoted CIS/6-31++G(d,p) in the terminology of Gaussian,[17] starting at the vertical geometry, that is, the equilibrium geometry of the ground-state. Because the optimization procedure moves downhill in energy along (or very close to) the path of steepest descent, it provides an efficient way of identifying a barrier-free dissociation path, should one exist, as well as the dissociation products. Of course, a much more extensive

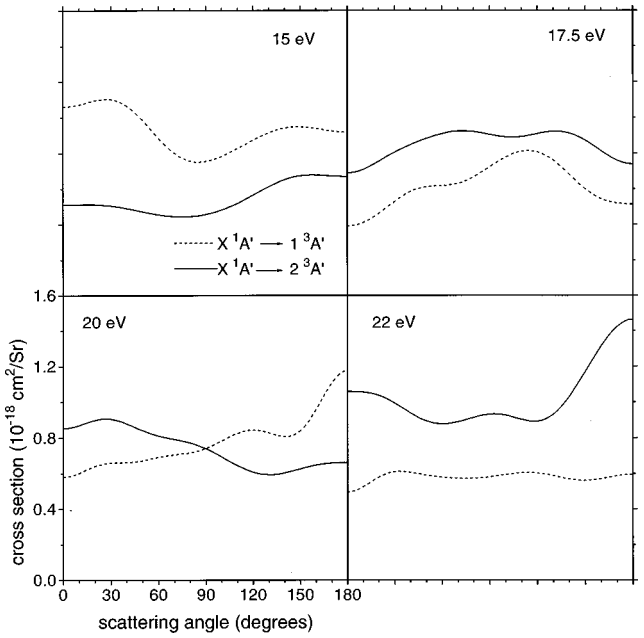

FIG. 7. Computed differential cross sections for electron-impact excitation to the $1\,^3A'$ (dashed line) and $2\,^3A'$ (solid line) excited states of C_2HF_5, at 15, 17.5, 20, and 22 eV.

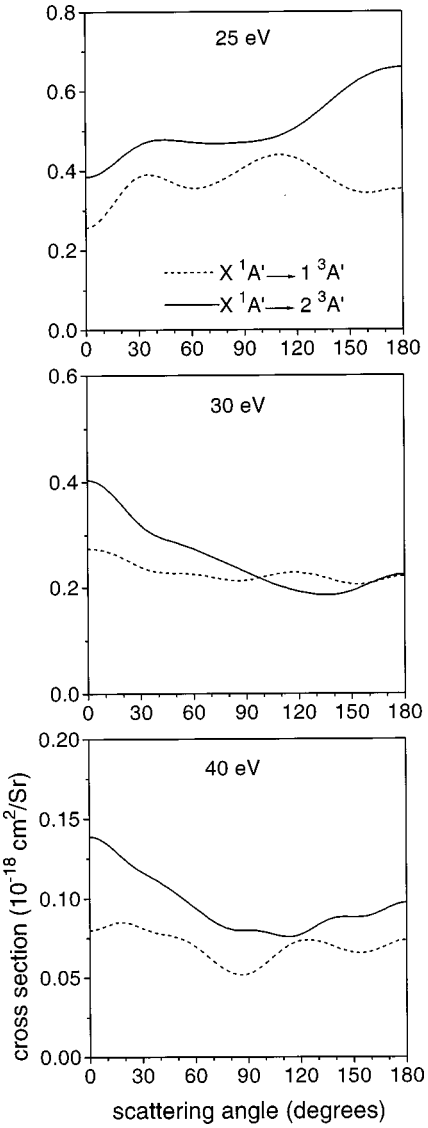

FIG. 8. Same as Fig. 7, at 25, 30, and 40 eV.

analysis would be needed to explore dissociation over barriers, alternative dissociation paths, nonadiabatic coupling to other surfaces, etc.

The SECI optimization indicated that the $1\,^3A'$ state dissociates without a barrier to C_2F_5+H. For the $2\,^3A'$ state, we were not able to obtain a definite result at the SECI level. We also carried out more elaborate calculations, using state-averaged complete active space (CAS) multiconfiguration self-consistent field (MCSCF) wave functions[35] computed with the program system MOLPRO;[36] in these calculations, the 6-31+G Gaussian basis set was used, and 26 orbitals were kept doubly occupied, leaving six electrons and six orbitals in the active space, for a (6,6) CAS in the usual notation. Although the CAS results confirmed the barrier-free dissociation of the $1\,^3A'$ state to C_2F_5+H, we were again unable to obtain a result for the $2\,^3A'$ state. However, examination of the gradient of the electronic potential at the vertical geometry indicates that the $2\,^3A'$ state may also dissociate to C_2F_5+H. Intersystem crossing from either triplet state to high vibrational levels of the $X\,^1A'$ ground state followed by dissociation is also possible. Experimental studies have shown that the ground state dissociates both to C_2F_4+HF (the lowest-energy channel) and to CHF_2+CF_3, with the latter channel dominating when sufficient energy is available for it to proceed.[37,38] We would therefore expect dissociation via coupling to the ground state mostly to produce CHF_2+CF_3.

Integral cross sections for electron-impact excitation to the $1\,^1A'$ and $2\,^1A'$ states are presented in Fig. 9. Comparison with Fig. 6 shows that the singlet cross sections are qualitatively similar to the triplet cross sections, having a double-peaked form, and also similar in magnitude. As in the case of the $1\,^3A'$ cross section, the main contribution to the peaks in the $1\,^1A'$ cross section comes from A' symmetry, though A'' also contributes. In the $2\,^1A'$ cross section, the lower peak occurs in A'' and the higher in A', reversing the pattern seen for $2\,^3A'$. As for the triplet excitations, these peaks are probably associated with core-excited shape resonances.

As discussed above, the singlet excitations are dipole-allowed and thus promoted by long-range collisions in which the passing charge interacts with the transition dipole. Even though this mechanism is not fully represented in our calculations, because we have not carried out the Born completion procedure, it probably has some effect even on the lower partial waves, and may help explain why the $1\,^1A'$ excitation, which has the larger oscillator strength, also has a larger electron-impact excitation cross section. We expect that inclusion of the dipole–Born correction would increase the magnitude of both the $1\,^1A'$ cross section significantly, particularly at the higher energies shown in Fig. 9; both the absolute and the percentage changes are expected to be smaller for the $2\,^1A'$ state because of its smaller transition dipole.

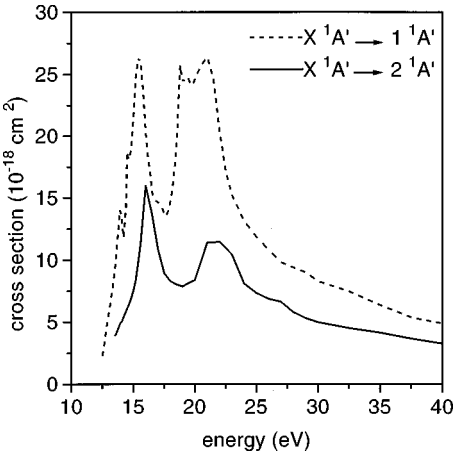

FIG. 9. Computed integral cross sections for electron-impact excitation to the $1\ ^1A'$ (dashed line) and $2\ ^1A'$ (solid line) excited states of C_2HF_5.

Differential excitation cross sections for the singlet states are shown in Figs. 10 and 11. The $2\ ^1A'$ cross section is nearly isotropic at most energies, while the $1\ ^1A'$ cross section possesses considerable structure, with the angular pattern evolving as the energy increases from threshold. Application of the dipole–Born correction would in both cases add a forward-scattering peak to the SMC DCS.

We were unable to obtain definitive results for the dissociation of the $^1A'$ excited states either at the SECI level or at the state-averaged (6,6) CAS level of approximation. However, as for the $2\ ^3A'$ state, some information can be gleaned from the potential gradients in each state at the vertical geometry, which we obtained from the CAS calculations. In the $1\ ^1A'$ state there is strong C–F repulsion within the CHF_2 moiety, suggesting that the state may dissociate to $CHFCF_3$+F, breaking C_s symmetry. The $2\ ^1A'$ state exhibits similar behavior, but the repulsive force is weaker and thus any conclusion even more tentative. Of course, another possibility for either state is radiative or nonradiative transition to vibrationally bound or unbound levels of the electronic ground state.

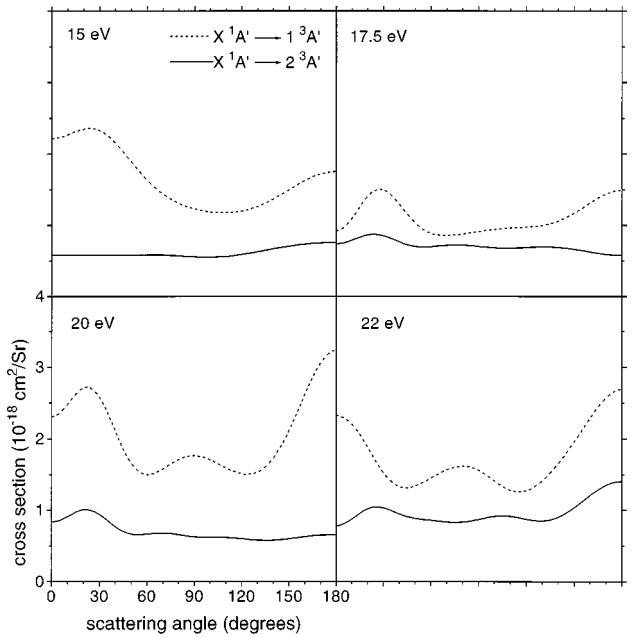

FIG. 10. Computed differential cross sections for electron-impact excitation to the $1\ ^1A'$ (dashed line) and $2\ ^1A'$ (solid line) excited states of C_2HF_5, at 15, 17.5, 20, and 22 eV.

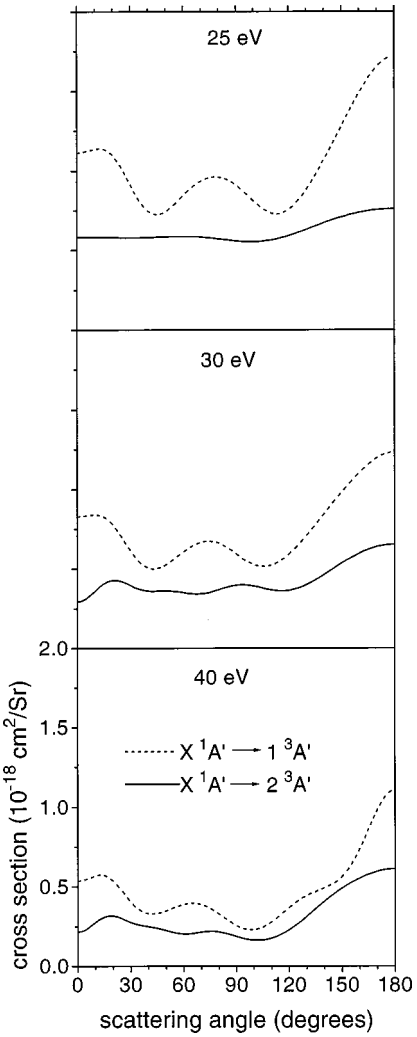

FIG. 11. Same as Fig. 10, at 25, 30, and 40 eV.

IV. CONCLUDING REMARKS

We presented elastic and inelastic cross sections for electron scattering by C_2HF_5. The elastic DCS is similar to that of C_2F_6 at higher energies. We found that the $1\ ^3A'$ state dissociates without a barrier into C_2F_5+H. Less definite conclusions could be drawn for the dissociation of the remaining states.

There is clearly much room for further work on C_2HF_5. Although we did not address here excitation to states of A'' symmetry, there is no reason to think that low-lying A'' are not important in electron-impact dissociation of C_2HF_5. Experimental work of all kinds, especially measurements of the total and elastic cross sections, would be quite helpful in understanding electron collisions with C_2HF_5 and the systematics of electron–haloethane collisions generally.

ACKNOWLEDGMENTS

M.H.F.B. acknowledges support from the Brazilian agency Conselho Nacional de Desenvolvimento Científico e Tecnológico (CNPq). C.W. and V.M. acknowledge support from the Department of Energy, Office of Energy Research. The authors acknowledge use of the facilities of the Center for Advanced Computing Research (CACR) at the California Institute of Technology and the valuable assistance of CACR staff, in particular Heidi Lorenz-Wirzba, Sharon Brunett, and Cris Windoffer.

[1] A. A. Christodoulides, L. G. Christophorou, R. Y. Pai, and C. M. Tung, J. Chem. Phys. **70**, 1156 (1979).
[2] R. Y. Pai, L. G. Christophorou, and A. A. Christodoulides, J. Chem. Phys. **70**, 1169 (1979).
[3] I. Sauers, L. G. Christophorou, and J. G. Carter, J. Chem. Phys. **71**, 3016 (1979).
[4] H. Tanaka, T. Masai, M. Kimura, T. Nishimura, and Y. Itikawa, Phys. Rev. A **56**, R3338 (1997).
[5] A. P. P. Natalense, M. H. F. Bettega, L. G. Ferreira, and M. A. P. Lima, Phys. Rev. A **59**, 879 (1999).
[6] R. Curik, F. A. Gianturco, and N. Sanna, J. Phys. B **33**, 615 (2000).
[7] M. T. do N. Varella, C. Winstead, V. McKoy, M. Kitajima, and H. Tanaka (unpublished).
[8] S. Agraharam, D. W. Hess, P. A. Kohl, and S. A. B. Allen, J. Vac. Sci. Technol. A **17**, 3265 (1999).
[9] P. D. Haaland (private communication).
[10] K. Takatsuka and V. McKoy, Phys. Rev. A **24**, 2473 (1981); **30**, 1734 (1984).
[11] M. A. P. Lima, L. M. Brescansin, A. J. R. da Silva, C. Winstead, and V. McKoy, Phys. Rev. A **41**, 327 (1990).
[12] C. Winstead and V. McKoy, Adv. At., Mol., Opt. Phys. **36**, 183 (1996).
[13] C. Winstead and V. McKoy, Comput. Phys. Commun. **128**, 386 (2000).
[14] B. Beagley, M. O. Jones, and P. Yavari, J. Mol. Spectrosc. **71**, 203 (1981).
[15] Q. Sun, C. Winstead, and V. McKoy, Phys. Rev. A **46**, 6987 (1992).
[16] M. J. Seaton, Proc. Phys. Soc. London **79**, 1105 (1962).
[17] GAUSSIAN 94, Revision D.4, M. J. Frisch, G. W. Trucks, H. B. Schlegel *et al.*, Gaussian, Inc., Pittsburgh, PA, 1995.
[18] M. W. Schmidt, K. K. Baldridge, J. A. Boatz *et al.*, J. Comput. Chem. **14**, 1347 (1993).
[19] A. Di Giacomo and C. P. Smyth, J. Am. Chem. Soc. **77**, 774 (1955).
[20] C. W. Meyer and G. Morrison, J. Phys. Chem. **95**, 3860 (1991).
[21] W. J. Hunt and W. A. Goddard, Chem. Phys. Lett. **3**, 414 (1969).
[22] V. McKoy, C. Winstead, and C.-H. Lee, J. Vac. Sci. Technol. A **16**, 324 (1998).
[23] C. Winstead and V. McKoy (unpublished).
[24] T. Takagi, L. Boesten, H. Tanaka, and M. A. Dillon, J. Phys. B **27**, 5389 (1994).
[25] T. N. Rescigno and B. H. Lengsfield, Z. Phys. D: At., Mol. Clusters **24**, 117 (1992).
[26] T. N. Rescigno, B. H. Lengsfield, C. W. McCurdy, and S. D. Parker, Phys. Rev. A **45**, 7800 (1992).
[27] A. P. P. Natalense, M. T. do N. Varella, M. H. F. Bettega, L. G. Ferreira, and M. A. P. Lima, J. Phys. B **32**, 5523 (1999).
[28] C. Winstead, Q. Sun, and V. McKoy, J. Chem. Phys. **98**, 1105 (1993).
[29] A. P. P. Natalense, M. H. F. Bettega, L. G. Ferreira, and M. A. P. Lima, Phys. Rev. A **52**, R1 (1995); M. T. do N. Varella, A. P. P. Natalense, M. H. F. Bettega, and M. A. P. Lima, *ibid.* **60**, 3684 (1999).
[30] W. A. Isaacs, C. W. McCurdy, and T. N. Rescigno, Phys. Rev. A **58**, 309 (1998).
[31] F. A. Gianturco, R. R. Lucchese, and N. Sanna, J. Chem. Phys. **104**, 6482 (1996).
[32] L. Boesten, H. Tanaka, A. K. Kobayashi, M. A. Dillon, and M. Kimura, J. Phys. B **25**, 1607 (1992).
[33] A. Mann and F. Linder, J. Phys. B **25**, 533 (1992).
[34] A. Mann and F. Linder, J. Phys. B **25**, 545 (1992).
[35] H.-J. Werner and P. J. Knowles, J. Chem. Phys. **82**, 5053 (1985); P. J. Knowles and H.-J. Werner, Chem. Phys. Lett. **115**, 259 (1985).
[36] MOLPRO is a package of *ab initio* programs written by H.-J. Werner and P. J. Knowles, with contributions from J. Almlöf, R. D. Amos, A. Berning *et al.*, Birmingham, UK, 1998.
[37] E. Tschuikow-Roux, G. E. Millward, and W. J. Quiring, J. Phys. Chem. **75**, 3493 (1971).
[38] S. Kato, Y. Makide, K. Takeuchi, and T. Tominaga, J. Phys. Chem. **88**, 3977 (1984).